JCTC Journal of Chemical Theory and Computation

An Atoms in Molecules Study of the Halogen Resonance Effect

Norberto Castillo and Russell J. Boyd*

Department of Chemistry, Dalhousie University, Halifax, N.S., Canada B3H 4J3

Received September 22, 2005

Abstract: We report a detailed study by means of the theory of atoms in molecules (AIM) of the resonance effect exhibited in systems where a halogen is adjacent to a carbon−carbon double bond. Moreover, we have carried out a comparable study of the respective saturated halohydrocarbons and hydrocarbons, as well as the related unsaturated hydrocarbons. The valence shell charge concentration (VSCC) of the atoms in systems that exhibit the halogen resonance effect is considerably different from that of the systems where only the electron withdrawing inductive effect is present. Our analysis of the bonded maximum charge concentration and the electronic properties at the bond critical points clearly indicate that the carbon−carbon double bond is strongly distorted as a result of the halogen resonance effect. Population analyses show that the halogen resonance effect is a donor effect, but the opposing electron-withdrawing inductive effect is stronger. Moreover, the analysis in terms of link points of the VSCCs of the carbons accounts for the observed position-dependence of electrophilic aromatic substitution in α- and β-halonaphthalenes.

1. Introduction

The electronic structure of certain classes of molecular species cannot be adequately described by a single Lewis structure. In some cases, the actual electronic structure is a weighted average of two or more Lewis structures, called resonance structures, and the molecule is known as a resonance hybrid. The concept of resonance is especially useful for systems containing delocalized electrons and has been used to explain many phenomena in chemistry including several types of reactions and the stability and physical properties of compounds.

The experimental observation that electrophilic substitution at the ortho and para positions of halobenzenes (C_6H_5X) is more facile than at the meta position is readily rationalized by a halogen resonance effect. Thus, interaction of a halogen lone pair with the p atomic orbitals that form the delocalized system of π bonds leads to the halonium ion structures shown in Chart 1. It is impossible to draw an equivalent resonance structure for the intermediate formed by electrophilic substitution at the meta position of a halobenzene.

Chart 1. Resonance Structures for the Intermediates Formed by Electrophilic Aromatic Substitution of Y^+ at the Ortho (a) and Para (b) Positions of a Halobenzene

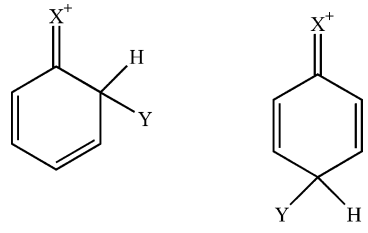

(a) (b)

Support for the standard interpretation of the experimental results is provided by molecular orbital (MO) calculations,[1] which clearly show a large contribution of the halogen to the π-bonding MOs. A similar effect is not observed in haloaliphatic compounds. In this paper, we report the first analysis of the halogen resonance effect by use of the theory of atoms in molecules (AIM).

2. The Theory of Atoms in Molecules and Resonance

The AIM theory uses well-defined quantities derived from the electron density to provide valuable insight into the

* Corresponding author tel.: (902) 494-8883; fax: (902) 494-1310; e-mail: russell.boyd@dal.ca.

10.1021/ct050238j CCC: $33.50
Published on Web 12/23/2005

Chart 2. Chemical Structures of Compounds Included in This Study, Where X = F, Cl, and Br

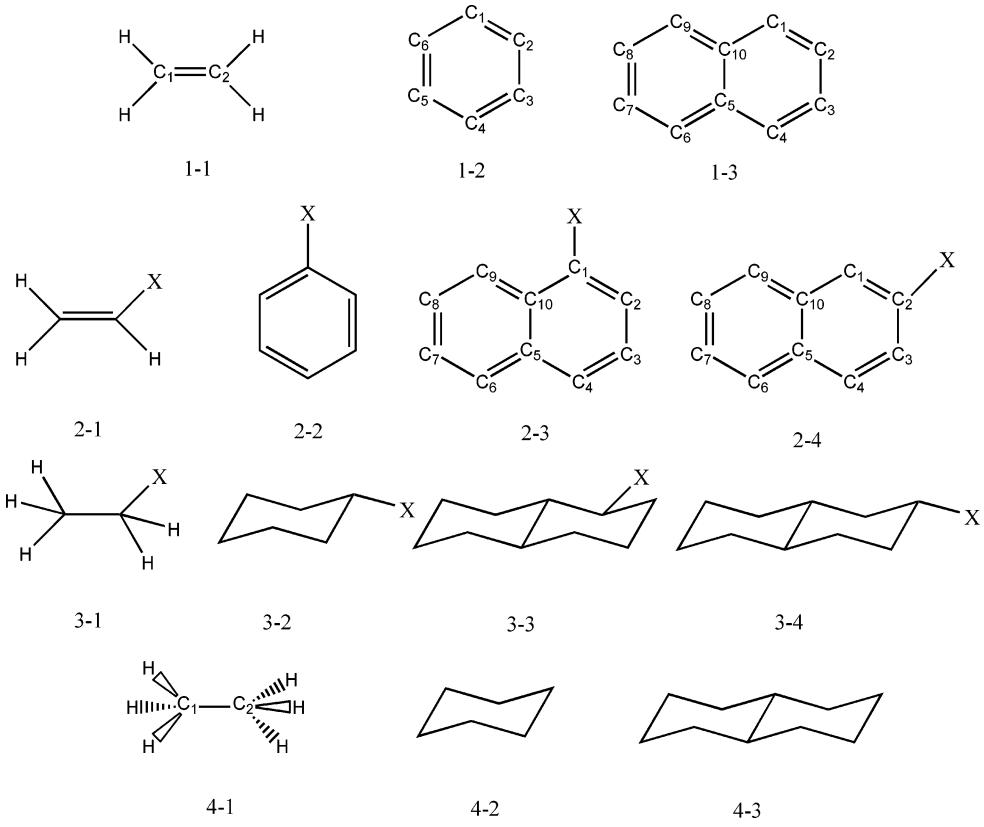

electronic structures and properties of molecules.[2−7] Bader[8] has studied the resonance effect in terms of $F^{\alpha}(\Omega,\Omega')$ and $F^{\beta}(\Omega,\Omega')$, which are the delocalization functions of electrons with α and β spins, respectively, between the basins of two atoms, Ω and Ω′. The delocalization function for α spin for a Slater determinantal wave function is given by

$$F^{\alpha}(\Omega,\Omega') = -\sum_i \sum_j \int \mathrm{d}r_1 \int \mathrm{d}r_2 \{\phi_i^*(r_1)\phi_j(r_1)\phi_j^*(r_2)\phi_i(r_2)\} = -\sum_{ij} S_{ij}(\Omega)\, S_{ji}(\Omega') \quad (1)$$

where the ϕ's are the α spin−orbitals and $S_{ij}(\Omega)$ denotes the overlap of a pair of α spin−orbitals over Ω (basin). An equivalent expression holds for β spin. Essentially, these delocalization functions measure the sharing of electrons between two atoms. The relationship between the delocalization index and bond order in the characterization of a chemical bond has been discussed previously.[9−12]

Bader et al.[13] used $F^{\alpha}(\Omega,\Omega')$ to quantify the contribution of each resonance structure in acyclic and cyclic hydrocarbons as well as the effect of substituents on delocalization in aromatic systems. More recently, González and Mosquera[14] reported a similar study in pyrimidinic bases but in terms of the delocalization index [$\delta(\Omega,\Omega')$], which is a more general parameter containing both delocalization functions:

$$\delta(\Omega,\Omega') = 2|F^{\alpha}(\Omega,\Omega')| + 2|F^{\beta}(\Omega,\Omega')| \quad (2)$$

Several other authors have used AIM to study the resonance effect in many different types of systems. For example, Okulik et al. have used AIM parameters to study the "three-center two-electron bonds" exhibited by isobutonium[15] and *n*-butonium[16] cations. Grabowski[17,18] and Gilli et al.[19] have used AIM analysis in terms of the electron density and the Laplacian at the bond critical points to explore the resonance-assisted hydrogen bonds in malonaldehyde and ketohydrazone−azoenol systems, respectively. Also, Borbulevych et al.[20] used the AIM theory to analyze substituent effects in 4-nitroaniline derivatives.

In this paper, we present a detailed AIM study of systems where the halogen is adjacent to a carbon−carbon double bond. Moreover, we have carried out a comparable study of the respective saturated halohydrocarbons and hydrocarbons as well as the related unsaturated hydrocarbons. The molecules included in this study are shown in Chart 2, where X = F, Cl, and Br. The first series consists of ethene (1-1), benzene (1-2), and naphthalene (1-3). The second series consists of their four monohalo derivatives. The third series consists of the saturated analogues of series 2, while the fourth series consists of the unsubstituted parent compounds of the third series. The emphasis of our study is on bond critical points, ellipticities, Laplacian topology, delocalization indexes, and population analysis for the main atoms and bonds associated with the resonance effect.

A secondary purpose of this paper is to perform an AIM study of electrophilic aromatic substitution in the halonaphthalenes in order to complement Bader and Chang's earlier study of benzene.[21] We use an analysis of the link points of the carbon valence shell charge concentrations (VSCCs) of the ring to predict the directing and activating-deactivating effects of halogens in naphthalene.

3. Computational Details

All molecules were fully optimized at the B3LYP/6-311++G(d,p) level using the Gaussian 03 package.[22] The characterization of the bond and ring critical points as well as the maximum charge concentrations was carried out using the EXTREME program, while the atomic populations were performed by PROAIM. Both programs belong to the AIMPAC package.[23,24] The AIMDELOC program was used to obtain the delocalization indexes.[25]

4. Results and Discussion

4.1. Valence-Shell Characterization of Chlorine in Compound Series 2 And 3. The characterization of the valence shell was carried out in terms of the (3, −3) critical points of L ($L = -\nabla^2\rho$), which represent the bonded and nonbonded maximum charge concentrations in the VSCC of an atom in a molecule. The locations of the (3, −3) critical points of L provide theoretical support for the bonded and nonbonded electron pairs of the Lewis model.[26−28] Figure 1 illustrates the locations of the (3, −3) critical points in the valence shell of chlorine in compound series 2 and 3. The position of each (3, −3) critical point is indicated by a vector whose origin is at the chlorine nucleus. To illustrate the distortion of the VSCC in each case, Figure 2 shows the contour map of the Laplacian for the plane that contains the halogen and the two carbons of chloroethane and chloroethene.

Figure 1 clearly shows that the chlorine VSCC exhibits two nonbonded maxima in series 2 and three nonbonded maxima in series 3. Moreover, the missing nonbonded maxima in series two are positioned optimally to delocalize the π cloud of the carbon−carbon double bonds. Figure 1 also illustrates that the other two nonbonded maxima are in the σ plane of the carbon−carbon double bonds, which is a favorable location for the delocalization of the missing nonbonded maximum charge concentration into the π cloud. Furthermore, Figure 2 shows contour lines connecting the VSCC of chlorine with the VSCC of carbon in chloroethene, signifying a greater distortion of the VSCCs of chlorine and carbon in chloroethene than in chloroethane. This suggests a greater sharing of electrons in the chlorine−carbon bond of chloroethene than that in chloroethane and also suggests that the halogen resonance effect is a donor effect.

Table 1 describes the VSCC of chlorine in compound series 2 and series 3 in terms of several electronic properties. The radii, $-\nabla^2\rho$, and ρ at the bonded maximum charge concentration of the chlorine VSCC are larger in series 2 than in series 3. The same trend holds for the nonbonded maximum charge concentrations, with the exception of the radii, which are slightly larger in series 3 than in series 2. The radii of the nonbonded maximum charge concentrations are smaller in series 2 than series 3, whereas $-\nabla^2\rho$ and ρ continue being larger. The decrease of the angle from series 2 to series 3 indicates the change of the chlorine VSCC from trigonal planar to tetrahedral. All these results support the fact that one nonbonded maximum is delocalized into the π cloud of the double bonds in series 2.

4.2. Comparison of the Fluorine and Bromine Valence Shells with Chlorine in Compound Series 2 and Series 3. The bonded maximum charge concentrations of the VSCCs of fluorine and bromine in series 2 and series 3 were not found at the level of theory used in this study. The results are listed in Table 2. It is possible that the maxima would be found at higher levels of calculation since it is known that the use of a triplet-ζ basis set is the minimum requirement to obtain consistent and topologically stable graphs of the Laplacian.[29]

The nonbonded maxima charge concentrations for fluorine and bromine have similar characteristics to that of chlorine. For example, the VSCCs for the two atoms exhibit two

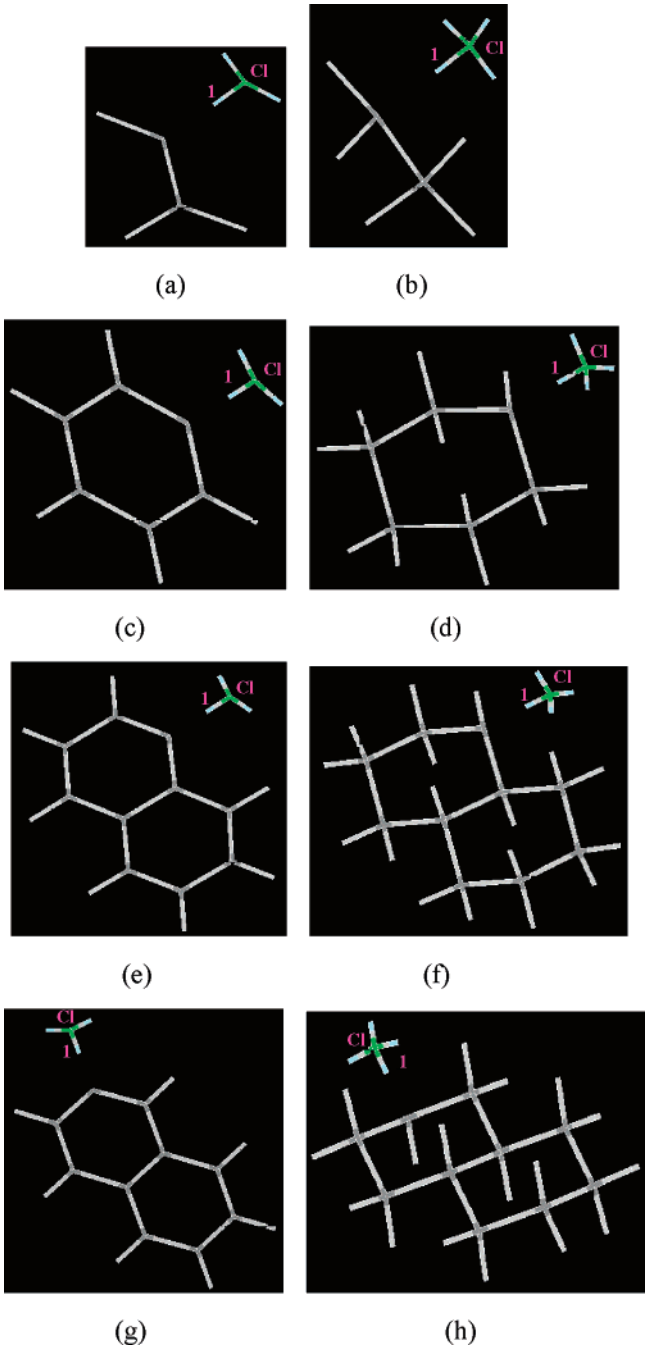

Figure 1. Location of the maximum charge concentrations of the VSCCs of chlorine in compound series 2 and series 3. In each molecule, the bonded maximum charge concentration is directed toward the carbon atom bonded to chlorine and is labeled by 1. Representations are as follows: (a) 2-1, (b) 3-1, (c) 2-2, (d) 3-2, (e) 2-3, (f) 3-3, (g) 2-4, and (h) 3-4.

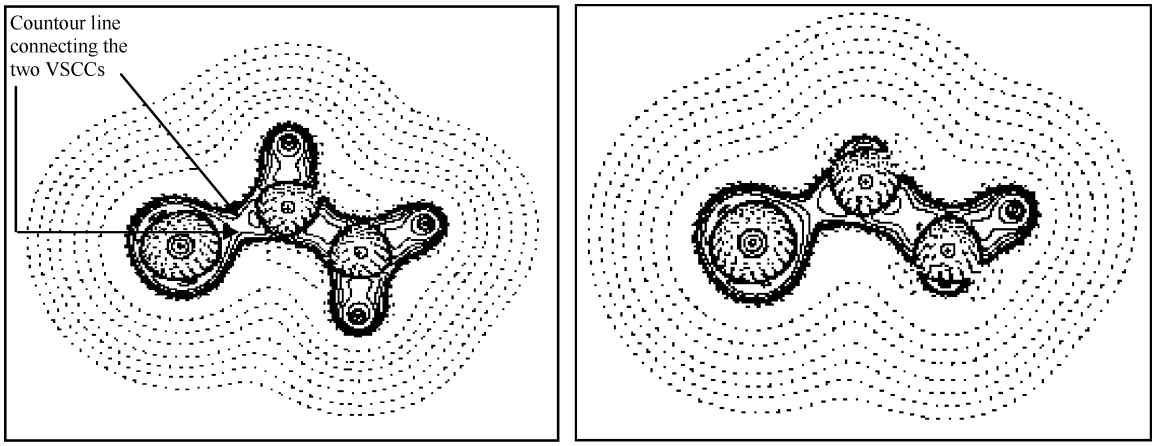

Figure 2. Contour map of the Laplacian of the electron density in the plane that contains the chlorine and the two carbons. (a) Chloroethene and (b) chloroethane. The chlorine nucleus is on the left side in both cases.

Table 1. Characterization of the Maximum Charge Concentrations in the VSCCs of Chlorine in Compound Series 2 and Series 3 in Terms of the Number of Bonded Maxima (# b), the Number of Nonbonded Maxima (# nb), Radius (r), $-\nabla^2\rho$, ρ, and Average Angles between Nonbonded Maxima[a]

	bonded maxima				nonbonded maxima				
molecule	# b	r	$-\nabla^2\rho \times 10^1$	$\rho \times 10^1$	# nb	r	$-\nabla^2\rho \times 10^1$	$\rho \times 10^1$	angle (nb−nb)
2-1	1	1.271	6.18	2.55	2	1.185	8.52	2.78	152.4
						1.185	8.50	2.78	
3-1	1	1.265	5.76	2.45	3	1.187	8.31	2.76	115.2
						1.187	8.31	2.76	
						1.187	8.30	2.76	
2-2	1	1.271	6.09	2.53	2	1.185	8.47	2.78	153.1
						1.185	8.47	2.78	
3-2	1	1.261	5.74	2.45	3	1.188	8.19	2.75	115.5
						1.188	8.21	2.75	
						1.188	8.21	2.75	
2-3	1	1.271	6.03	2.52	2	1.185	8.47	2.78	153.4
						1.185	8.49	2.78	
3-3	1	1.258	5.73	2.51	3	1.187	8.21	2.75	115.1
						1.188	8.19	2.75	
						1.187	8.21	2.75	
2-4	1	1.271	6.08	2.53	2	1.185	8.47	2.78	153.7
						1.185	8.47	2.78	
3-4	1	1.261	5.73	2.45	3	1.188	8.19	2.75	115.3
						1.188	8.21	2.75	
						1.187	8.21	2.75	

[a] Radius in angstroms, $-\nabla^2\rho$ and ρ in atomic units, and angles in degrees.

nonbonded maxima in series 2, whereas there are three nonbonded maxima in series 3. Also, the nonbonded maximum charge concentrations in series 2 are in a favorable location for the delocalization of the missing nonbonded maximum charge concentration into the π cloud. The radius of the nonbonded maximum charge concentration increases from series 2 to series 3, whereas $-\nabla^2\rho$, ρ, and the angles decrease. A decrease of almost 75% in the $-\nabla^2\rho$ value for the nonbonded maximum charge concentration in the bromine case is noteworthy. This result is expected because bromine is considerably larger than chlorine and fluorine, and any displacement of the same amount of electron charge involves larger volumes. Therefore, the concentration of ρ decreases more significantly than in the cases of chlorine and fluorine.

4.3. Characterization of the Bonded Maximum Charge Concentrations of the Carbons Connected to Halogens. As was shown above, the VSCCs of the halogens are significantly altered by the resonance effect. Hence, it can be expected that the VSCCs of the carbon atoms joined to the halogen will also exhibit detectable modifications. Therefore, we analyzed the VSCCs of these carbon atoms for series 2 and series 3 with the three different halogens. Table 3 provides the results for the bonded maximum charge concentration of the carbon bonded to the halogens. As can be seen in the table, the systems with the resonance effect

Table 2. Characterization of the Nonbonded Maximum Charge Concentrations in the VSCCs of Fluorine and Bromine in Series 2 and Series 3 in Terms of the Number of Nonbonded Maxima (# nb), Radius (r), $-\nabla^2\rho$, ρ, and Average Angles between Nonbonded Maxima[a]

Nonbonded Maxima											
	fluorine						bromine				
molecule	# nb	r	$-\nabla^2\rho\times10^2$	$\rho\times10^1$	angle (nb−nb)	molecule	# nb	r	$-\nabla^2\rho$	r	angle (nb−nb)
2-1	2	0.569	9.34	1.52	157.0	2-1	2	1.567	0.82	1.65	158.9
		0.569	9.31	1.52				1.568	0.82	1.65	
3-1	3	0.571	9.06	1.50	116.2	3-1	3	1.574	0.21	1.62	117.1
		0.571	9.06	1.50				1.574	0.19	1.62	
		0.571	9.07	1.50				1.574	0.19	1.62	
2-2	2	0.569	9.28	1.52	155.7	2-2	2	1.567	0.76	1.65	159.8
		0.569	9.28	1.51				1.567	0.76	1.65	
3-2	3	0.571	9.00	1.50	116.6	3-2	3	1.577	0.16	1.61	117.3
		0.571	8.98	1.50				1.576	0.03	1.61	
		0.571	9.00	1.50				1.576	0.03	1.61	
2-3	2	0.569	9.26	1.52	156.1	2-3	2	1.566	0.94	1.66	159.8
		0.569	9.26	1.52				1.566	0.77	1.65	
3-3	3	0.571	9.01	1.50	116.0	3-3	3	1.576	0.11	1.61	116.7
		0.571	8.96	1.50				1.578	0.29	1.60	
		0.571	8.98	1.50				1.575	0.09	1.62	
2-4	2	0.569	9.28	1.52	156.6	2-4	2	1.567	0.79	1.65	159.3
		0.569	9.28	1.52				1.567	0.77	1.65	
3-4	3	0.571	8.97	1.50	116.6	3-4	3	1.577	0.16	1.61	117.2
		0.571	9.00	1.50				1.576	0.03	1.61	
		0.571	9.00	1.50				1.576	0.03	1.61	

[a] Radius in angstroms, $-\nabla^2\rho$ and ρ in atomic units, and angles in degrees.

Table 3. Characterization of the Carbon−Halogen Bonded Maximum Charge Concentrations in the VSCC of the Carbon Connected to the Halogen (Fluorine, Chlorine, or Bromine) in Terms of Radius, $-\nabla^2\rho$, and ρ for Series 2 and Series 3[a]

fluorine				chlorine				bromine			
molecule	r	$-\nabla^2\rho\times10^1$	$\rho\times10^1$	molecule	r	$-\nabla^2\rho\times10^1$	$\rho\times10^1$	molecule	r	$-\nabla^2\rho\times10^1$	$\rho\times10^1$
2-1	1.043	3.47	2.63	2-1	1.035	4.99	2.13	2-1	1.027	4.81	2.02
3-1	1.053	2.64	2.29	3-1	1.054	3.84	1.89	3-1	1.049	3.53	1.79
2-2	1.044	3.51	2.62	2-2	1.034	4.95	2.11	2-2	1.026	4.80	2.01
3-2	1.052	2.45	2.23	3-2	1.054	3.61	1.85	3-2	1.049	3.33	1.75
2-3	1.045	3.43	2.61	2-3	1.035	4.84	2.10	2-3	1.027	4.68	1.99
3-3	1.054	2.37	2.21	3-3	1.055	3.53	1.83	3-3	1.050	3.20	1.73
2-4	1.044	3.51	2.62	2-4	1.034	4.94	2.11	2-4	1.026	4.80	2.01
3-4	1.053	2.44	2.23	3-4	1.055	3.59	1.84	3-4	1.050	3.31	1.75

[a] Radius in angstroms and $-\nabla^2\rho$ and ρ in atomic units.

(series 2) exhibit smaller radii and greater values of $-\nabla^2\rho$ and ρ at the maximum charge concentration of the carbon bonded to the halogen than those without the resonance effect (series 3). This fact can be explained by the delocalization of the nonbonded charge concentration in the carbon−halogen bond. The resonance effect plays a similar role in the unsaturated aliphatic halohydrocarbon to that of the aromatic halohydrocarbon. There are no appreciable differences with respect to the radius, $-\nabla^2\rho$, and ρ between the haloethene (2-1), the halobenzene (2-2), and the halonaphthalenes (2-3 and 2-4), respectively. Fluorine produces the smallest value of $-\nabla^2\rho$ and the largest value of ρ at the bonded maximum charge concentration of the carbon bonded to the halogen.

We analyzed the carbon connected to the halogen in series 2 and series 3 in terms of the bonded charge concentration contained in the carbon−carbon bond in order to investigate the halogen resonance effect on the carbon−carbon double bond in series 2. Also, we characterized the respective bonded charge concentrations of the carbons for the nonhalogen systems (series 1 and series 4) to make illustrative comparisons. Table 4 provides the results. The VSCC of the carbon connected to the halogen in series 2 and series 3 exhibits a bonded maximum charge concentration contained in the carbon−carbon bond with smaller radii than the nonhalogen systems (series 1 and series 4). The radii are even smaller in cases where the halogen resonance effect exists (series 2). Moreover, series 2 exhibits the greatest values of $-\nabla^2\rho$ and ρ at these bonded maximum charge concentrations. The values of $-\nabla^2\rho$ and ρ for nonhalogen unsaturated systems (series 1) are between the two types of halogen systems (series 2 and series 3). Fluorine produces smaller radii and larger values of $-\nabla^2\rho$ and ρ in its compounds than chlorine and bromine. Slight differences are

Table 4. Characterization of the Carbon−Carbon Bonded Maximum Charge Concentrations in the VSCCs of the Carbon Connected to the Halogen (Fluorine, Chlorine, or Bromine) in Terms of Radius, $-\nabla^2\rho$, and ρ for All Four Series[a]

fluorine				chlorine				bromine			
molecule	*r*	$-\nabla^2\rho$	$\rho \times 10^1$	molecule	*r*	$-\nabla^2\rho$	$\rho \times 10^1$	molecule	*r*	$-\nabla^2\rho$	$\rho \times 10^1$
1-1	0.987	1.14	3.53	1-1	0.987	1.14	3.53	1-1	0.987	1.14	3.53
2-1	0.958	1.28	3.71	2-1	0.968	1.21	3.63	2-1	0.970	1.19	3.61
3-1	0.966	1.03	2.94	3-1	0.970	0.98	2.88	3-1	0.971	0.97	2.88
4-1	0.996	0.82	2.68	4-1	0.996	0.82	2.68	4-1	0.996	0.82	2.68
1-2	0.983	1.06	3.25	1-2	0.983	1.06	3.25	1-2	0.983	1.06	3.25
2-2	0.958	1.20	3.43	2-2	0.965	1.13	3.34	2-2	0.967	1.11	3.32
3-2	0.962	1.05	2.96	3-2	0.966	1.00	2.91	3-2	0.967	0.99	2.90
4-2	0.991	0.85	2.72	4-2	0.991	0.85	2.72	4-2	0.991	0.85	2.72
1-3 (C_1)	0.982	1.09	3.34	1-3 (C_1)	0.982	1.09	3.34	1-3 (C_1)	0.982	1.09	3.34
2-3	0.957	1.23	3.52	2-3	0.965	1.15	3.43	2-3	0.967	1.13	3.41
3-3	0.962	1.05	2.96	3-3	0.965	1.00	2.92	3-3	0.966	0.99	2.90
4-3 (C_1)	0.991	0.85	2.72	4-3 (C_1)	0.991	0.85	2.72	4-3 (C_1)	0.991	0.85	2.72
1-3 (C_2)	0.983	1.08	3.34	1-3 (C_2)	0.983	1.08	3.34	1-3 (C_2)	0.983	1.08	3.34
2-4	0.957	1.23	3.51	2-4	0.966	1.15	3.43	2-4	0.968	1.13	3.41
3-4	0.962	1.05	2.96	3-4	0.966	1.00	2.91	3-4	0.967	0.99	2.90
4-3 (C_2)	0.991	0.85	2.72	4-3 (C_2)	0.991	0.85	2.72	4-3 (C_2)	0.991	0.85	2.72

[a] Radius in angstroms and $-\nabla^2\rho$ and ρ in atomic units.

Table 5. Ellipticity (ϵ), ρ, and $-\nabla^2\rho$ of the Carbon−Halogen (Fluorine, Chlorine, and Bromine) Bonds for Series 2 and Series 3[a]

	fluorine				chlorine				bromine			
molecule	bond	$\epsilon \times 10^2$	$\rho \times 10^1$	$-\nabla^2\rho \times 10^1$	bond	$\epsilon \times 10^2$	$\rho \times 10^1$	$-\nabla^2\rho \times 10^1$	bond	$\epsilon \times 10^2$	$\rho \times 10^1$	$-\nabla^2\rho \times 10^1$
2-1	C−F	7.36	2.49	1.44	C−Cl	5.09	1.94	2.84	C−Br	6.22	1.57	1.47
3-1	C−F	3.25	2.23	0.37	C−Cl	1.40	1.67	1.87	C−Br	1.26	1.36	1.05
2-2	C−F	6.58	2.48	1.21	C−Cl	5.61	1.91	2.72	C−Br	6.37	1.55	1.44
3-2	C−F	1.02	2.18	0.63	C−Cl	0.86	1.61	1.64	C−Br	0.85	1.31	0.92
2-3	C−F	5.66	2.47	1.31	C−Cl	5.73	1.90	2.64	C−Br	6.38	1.53	1.39
3-3	C−F	0.46	2.16	0.64	C−Cl	0.90	1.60	1.58	C−Br	0.76	1.28	0.84
2-4	C−F	6.12	2.48	1.20	C−Cl	5.71	1.91	2.72	C−Br	6.47	1.55	1.45
3-4	C−F	1.17	2.18	0.65	C−Cl	0.90	1.61	1.63	C−Br	0.86	1.31	0.91

[a] ϵ, ρ, and $-\nabla^2\rho$ in atomic units.

found between unsaturated aliphatic and aromatic compounds in terms of $-\nabla^2\rho$ and ρ values. For example, ethane (1-1) and chloroethene (2-1) exhibit larger radii and greater values of $-\nabla^2\rho$ and ρ than benzene (1-2) and chlorobenzene (2-2), respectively.

4.4. Characterization of the Carbon−Halogen and Carbon−Carbon Bonds. It is well-established that the electronic properties at the bond critical point provide extensive information about a chemical bond.[2] Therefore, we carried out the characterization of the bond critical points at the carbon−halogen bond in series 2 and series 3 for the three halogens in terms of ellipticity, ρ, and $-\nabla^2\rho$. The bond critical point at the carbon−carbon bond was also characterized, and a comparison with the carbon−carbon bonds in series 1 and series 4 was carried out. The data in Table 5 indicate that the ellipticities of carbon−halogen bonds are greater in systems where the resonance effect exists. For example, the ellipticity of the carbon−chlorine bond in chloroethene (2-1) is 5.09×10^{-2} au (atomic units), which is greater than the 1.40×10^{-2} au exhibited in chloroethane (3-1). Moreover, the ellipticities are greater in halogen unsaturated aliphatic systems (2-1) than in halogen aromatic systems (2-2, 2-3, and 2-4) for chlorine and bromine. The opposite behavior is observed for fluorine.

The electron density at the bond critical point is also greater in systems where the halogen resonance effect is present (series 2). Fluorine produces the greatest value of ρ at the bond critical point. There are no appreciable differences between halogen unsaturated aliphatic and halogen aromatic systems in terms of ρ at the carbon−halogen bond critical point. Similar behavior is observed for $-\nabla^2\rho$ except that chlorine produces the greatest values. $-\nabla^2\rho$ values for halogen unsaturated aliphatic systems are slightly greater than those of halogen aromatic systems for the three halogens.

Table 6 shows that series 2 exhibits greater values of ellipticities in the carbon−carbon double bond than series 1. For example, the ellipticity at the carbon−carbon double bond in fluoroethene (2-1) is 4.20×10^{-1} au, which is greater than the 3.32×10^{-1} au exhibited in ethene (1-1). This observation can be explained by the delocalization of one nonbonded maximum charge concentration by the resonance effect through the carbon−halogen bond, which contributes to an increase in the electron density in the π plane of the whole system.

ρ and $-\nabla^2\rho$ at the bond critical point of the carbon−carbon double bond are slightly greater in series 2 than in series 1, with fluorine yielding the greatest differences. Moreover, the carbon−carbon bond in series 2 exhibits considerably greater

Table 6. Ellipticity (ϵ), ρ, and $-\nabla^2\rho$ of the Carbon−Carbon Bond Adjacent to the Halogen for All Four Series[a]

fluorine				chlorine				bromine			
molecule	*e*	$\rho \times 10^1$	$-\nabla^2\rho \times 10^1$	molecule	*e*	$\rho \times 10^1$	$-\nabla^2\rho \times 10^1$	molecule	*e*	$\rho \times 10^1$	$-\nabla^2\rho \times 10^1$
1-1	3.3210^{-1}	3.44	10.27	1-1	3.3210^{-1}	3.44	10.27	1-1	3.3210^{-1}	3.44	10.27
2-1	4.2010^{-1}	3.52	10.72	2-1	3.7910^{-1}	3.47	10.37	2-1	3.6810^{-1}	3.47	10.34
3-1	4.1510^{-2}	2.54	6.13	3-1	1.6710^{-2}	2.48	5.80	3-1	9.3710^{-3}	2.48	5.78
4-1	2.2410^{-5}	2.41	5.49	4-1	2.2410^{-5}	2.41	5.49	4-1	2.2410^{-5}	2.41	5.49
1-2	2.0010^{-1}	3.08	8.59	1-2	2.0010^{-1}	3.08	8.59	1-2	2.0010^{-1}	3.08	8.59
2-2	2.6110^{-1}	3.17	9.10	2-2	2.3210^{-1}	3.10	8.65	2-2	2.2410^{-1}	3.10	8.60
3-2	4.3810^{-2}	2.53	6.03	3-2	2.0710^{-2}	2.47	5.70	3-2	1.4010^{-2}	2.47	5.67
4-2	6.6110^{-3}	2.39	5.31	4-2	6.6110^{-3}	2.39	5.31	4-2	6.6110^{-3}	2.39	5.31
1-3	2.4210^{-1}	3.20	9.13	1-3	2.4210^{-1}	3.20	9.13	1-3	2.4210^{-1}	3.20	9.13
2-3	3.0910^{-1}	3.28	9.58	2-3	2.7710^{-1}	3.21	9.14	2-3	2.6910^{-1}	3.20	9.08
3-3	4.4510^{-2}	2.53	6.04	3-3	2.4410^{-2}	2.48	5.73	3-3	1.5210^{-2}	2.46	5.65
4-3	5.9710^{-3}	2.40	5.34	4-3	5.9710^{-3}	2.40	5.34	4-3	5.9710^{-3}	2.40	5.34
1-3	2.4210^{-1}	3.20	9.13	1-3	2.4210^{-1}	3.20	9.13	1-3	2.4210^{-1}	3.20	9.13
2-4	3.1310^{-1}	3.28	9.59	2-4	2.8110^{-1}	3.22	9.17	2-4	2.7210^{-1}	3.21	9.12
3-4	4.3010^{-2}	2.53	6.04	3-4	1.9910^{-2}	2.48	5.72	3-4	1.3110^{-2}	2.47	5.69
4-3	5.9710^{-3}	2.40	5.34	4-3	5.9710^{-3}	2.40	5.34	4-3	5.9710^{-3}	2.40	5.34

[a] ϵ, ρ, and $-\nabla^2\rho$ in atomic units.

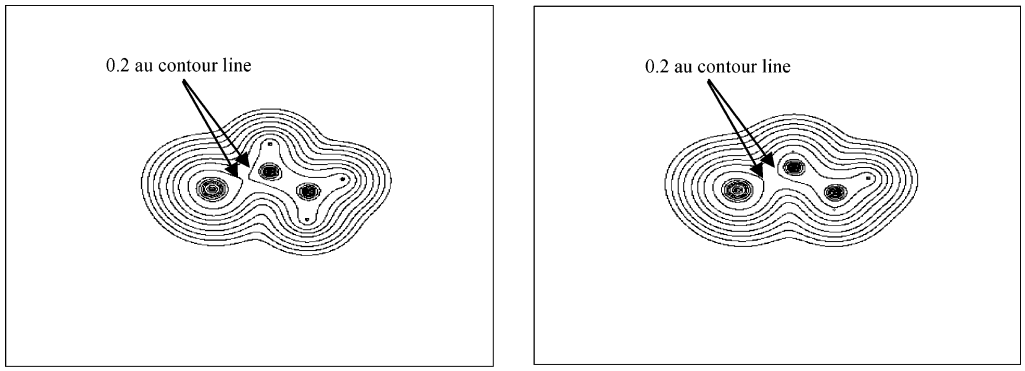

Figure 3. Contour map of the electron density in the plane that contains chlorine and the two carbons. (a) Chloroethene and (b) chloroethane.

values of ρ and $-\nabla^2\rho$ at the bond critical point than those in series 3. For example, fluoroethene (2-3) exhibits values of 3.52 and 10.72 au (ρ and $-\nabla^2\rho$), which are greater than the 2.54 and 6.13 au exhibited in fluoroethane, respectively. These facts can only be explained by the halogen resonance effect.

Furthermore, Figure 3 shows the contour map of the electron density in the plane that contains the halogen and the two carbons in chloroethane and chloroethene. Greater distortion of the 0.2 au contour line in chloroethene than that of chloroethane is clearly evident. Therefore, the halogen resonance effect produces a greater amount of charge in the area between the two atoms, which further demonstrates the donor character of the halogen resonance effect.

The ring critical points were also analyzed for the cyclic systems. The three halogens do not produce any appreciable effects on ρ and $-\nabla^2\rho$ at the ring critical points. Their values are very similar to those of the nonhalogen systems. Therefore, the presence of the halogens in the systems does not make any appreciable difference in the characteristics of the ring critical points whether the resonance effect exists or not.

4.5. Population Analysis. Table 7 lists the populations of the halogens and their adjacent carbons in series 2 and series 3. Clearly, the populations of chlorine and bromine in series 2 are smaller than those in series 3, whereas the population of fluorine remains constant at 9.62 au. Notice that the populations of chlorine and bromine are still greater than their respective atomic numbers (17 and 35). This suggests that the electron-withdrawing inductive effect of the halogens is stronger than the donor resonance effect. However, the fluorine systems do not follow the same behavior.

The populations of the carbons adjacent to the halogens are always greater in series 2 than in series 3. This is an expected result and restates the donor character of the halogen resonance effect. The resonance effect produced by the delocalization of one nonbonded maximum charge concentration of the VSCC of the halogens in series 2 donates charge to the adjacent carbon, increasing its population. It makes the populations of the carbons adjacent to the halogen in series 2 greater than that of the respective carbons in series 3 where only the electron-withdrawing inductive is present.

Table 7. Populations of the Halogens and Their Adjacent Carbons in Series 2 and Series 3[a]

		Population		
molecule	atoms	fluorine	chlorine	bromine
2-1	halogen	9.62	17.21	35.07
	carbon	5.56	5.97	6.11
3-1	halogen	9.62	17.28	35.18
	carbon	5.49	5.88	5.99
2-2	halogen	9.62	17.22	35.08
	carbon	5.55	5.96	6.10
3-2	halogen	9.62	17.30	35.20
	carbon	5.52	5.89	5.994
2-3	halogen	9.62	17.22	35.08
	carbon	5.55	5.96	6.10
3-3	halogen	9.62	17.30	35.21
	carbon	5.46	5.96	6.00
2-4	halogen	9.62	17.22	35.08
	carbon	5.55	5.96	6.10
3-4	halogen	9.62	17.30	35.20
	carbon	5.519	5.89	5.99

[a] Populations in atomic units.

Table 8. Delocalization Indexes for the Bonded Halogen−Carbon [δ(X,C)] in Series 2 and Series 3[a]

molecule	fluorine	chlorine	bromine
2-1	0.850	1.125	1.158
3-1	0.813	1.028	1.051
2-2	0.826	1.092	1.121
3-2	0.787	0.985	1.003
2-3	0.823	1.087	1.114
3-3	0.784	0.980	0.989
2-4	0.825	1.092	1.122
3-4	0.786	0.984	1.001

[a] Delocalization indexes in atomic units.

4.6. Delocalization Indexes. As explained above, δ(X,C) measures the sharing of electrons between a halogen and carbon. δ(X,C) is clearly greater in series 2 than in series 3 for chlorine and bromine (Table 8). The same behavior is observed in the case of fluorine, although the difference is not as great. These facts support the donor character of the halogen resonance effect in series 2, which produces a higher sharing of electrons between the three halogens and their bonded carbon than in series 3. On the other hand, fluorine and bromine exhibit the lowest and largest values of δ(X,C), respectively. In fact, the sharing of electrons between halogens and their bonded carbons in our systems is inversely related to the eletronegativity difference between the halogen and its bonded carbon. For example, δ(Br,C) is greater than δ(F,C) and δ(Cl,C) in both series, and the electronegativity difference increases from Br−C to F−C.

4.7. Electrophilic Aromatic Substitution in the α- and β-Halonaphthalenes. In their study of electrophilic aromatic substitution, Bader and Chang[21] showed that the Laplacian values at the saddle points, which link the carbon−carbon bonded charge concentration in substituted benzenes, predict the observed directing and activating−deactivating effects. These so-called link points exhibit the second-highest charge concentration of the VSCC of the atoms (second to the maximum charge concentration). In benzene, these points

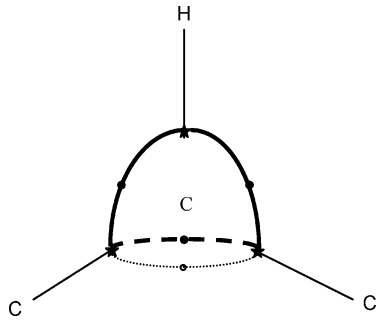

Figure 4. Atomic graphs describing the VSCC of a carbon in benzene. The maximum charge concentrations and link points are denoted by stars and dots, respectively. The solid link line is in the plane, the dashed link line is above the plane, and the gray link line is below the plane.

are above and below the plane of the ring. Therefore, it is reasonable to think of them as possible sites for electrophilic attack. The location of these link points in benzene is illustrated in Figure 4. In this paper, we have carried out a similar study of electrophilic aromatic substitution in the α- and β-halonaphthalenes.

As in the benzene case, there are two saddle points that link the two carbon−carbon bonded charge concentrations in the halonaphthalenes (one above and another below the plane of the ring). However, the saddle points which link the hydrogen−carbon maximum bonded charge concentrations are not always in the plane of the ring as in benzene (Figure 4). All carbons of the ring except the bridging carbons in the halonaphthalenes exhibit one hydrogen−carbon link point in the plane of the ring. Also, they exhibit two hydrogen−carbon link points out of the plane of the ring, one above and one below. It can be understood that one of the hydrogen−carbon link points that is in the plane in benzene is split into two hydrogen−carbon link points in the halonaphthalenes because of the lower symmetry. The location of the split of the link points alternates along the carbon chain. For example, there are four hydrogen−carbon link points in the region between C_1 and C_2 (the split of hydrogen−carbon link points for each carbon), and it repeats in the regions between C_3 and C_4, C_6 and C_7, and C_8 and C_9. On the other hand, there are two hydrogen−carbon link points in the region between C_2 and C_3 (the hydrogen−carbon link point in the plane for each carbon), and it repeats in the region between C_7 and C_8. Figure 5 illustrates the location of the link points in the α- and β-halonaphthalenes, and Table 9 provides $-\nabla^2\rho$ values of the carbon−carbon link points for the α- and β-halonaphthalenes. (The analysis of the hydrogen−carbon link points is not reported because it does not provide further insight. Their properties do not change appreciably throughout the ring, and also, they are generally similar to those of naphthalene for each halogen. Furthermore, their $-\nabla^2\rho$ values are noticeably lower than those for carbon−carbon link points. Thus, we focus on the carbon−carbon link points because they should play a major role as sites for electrophilic attack. We performed our analysis in terms of $-\nabla^2\rho$ to be consistent with the common practice in the literature, but it must be noted that the opposite convention was used by Bader and Chang.[21])

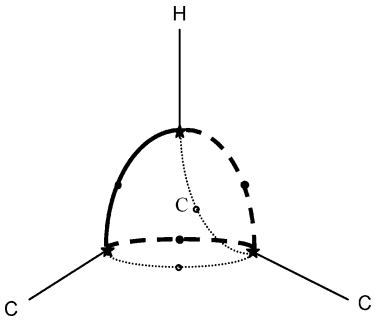

Figure 5. Atomic graphs describing the VSCC of a carbon in the halonaphthalenes. The maximum charge concentrations and link points are denoted by stars and dots, respectively. The solid link line is in the plane, the dashed link line is above the plane, and the gray link line is below the plane.

Table 9. Values of $-\nabla^2\rho$ for Carbon−Carbon Link Points in α- and β-Halonaphthalene[a]

α-halogen	F	Cl	Br	β-halogen	F	Cl	Br
C_2	0.159	0.150	0.149	C_1	0.165	0.156	0.154
C_3	0.135	0.136	0.136	C_3	0.150	0.146	0.146
C_4	0.145	0.139	0.136	C_4	0.136	0.136	0.137

[a] $-\nabla^2\rho$ in atomic units.

Experimental studies of electrophilic aromatic substitution[30] indicate that halogens at the α position (C_1) in naphthalene are C_2- and C_4-directing, whereas halogens at the β position (C_2) are C_1- and C_3-directing. As can be seen in the table, the link points with the largest values of $-\nabla^2\rho$ are in the VSCCs of C_2 and C_4 in the case of the α-halonaphthalenes. α-fluoronaphthalene exhibits the greatest values, 0.159 for C_2 and 0.145 for C_4, whereas α-bromonaphthalene exhibits the lowest values, 0.149 for C_2 and 0.136 for C_4. Thus, the electrophilic attack will preferentially occur at C_2 and C_4, following the trend F > Cl > Br as demonstrated by experiments. However, our results are not absolutely consistent with experimental results[30] because they predict that the electrophilic attack will be more preferentially directed to position C_2 than to position C_4 in the α-halonaphthalenes. Also, they predict a similar tendency of electrophilic aromatic substitution at the C_3 and C_4 positions except for the case of fluorine, where there is a noticeable preference of C_4 over C_3. The analysis for β-halonaphthalenes indicates a preference for C_1 over C_3 with the same trend as that observed in the α-halonaphthalenes (F > Cl > Br). These results are consistent with experimental results. Furthermore, the results predict faster electrophilic aromatic substitution at the C_1 position of the β-halonaphthalenes than at the C_2 position of the α-halonaphthalenes. These results are also consistent with experimental results.[30]

5. Conclusions

The VSCCs of the halogens in compounds where the halogens are bonded to a carbon−carbon single bond exhibit three nonbonded maximum charge concentrations (series 3). The location of these maxima can be considered to be tetrahedral. However, the VSCCs of the halogens bonded to a carbon−carbon double bond exhibit two nonbonded maximum charge concentrations in the sp^2 plane of the carbons (series 2). This suggests an overlapping or delocalization of one of the nonbonded maximum charge concentrations of the halogen into the π cloud of the carbon−carbon double bond by a resonance effect. The systems with the halogen resonance effect exhibit smaller radii and larger values of $-\nabla^2\rho$ and ρ at the maximum charge concentrations of the halogens than those in the systems where only the electron-withdrawing inductive effect of the halogen is acting.

In the case of the sp^2 carbons bonded to the halogen in series 2, their maximum charge concentrations bonded to the halogen exhibit smaller radii and greater values of $-\nabla^2\rho$ and ρ than those of the sp^3 carbons bonded to the halogen in series 3. Moreover, the maximum charge concentrations of the sp^2 carbons bonded to the other carbon that forms the carbon−carbon double bond in series 2 exhibit similar radii (in general, slightly smaller) and greater values of $-\nabla^2\rho$ and ρ than those of the sp^3 carbons bonded to the halogen in series 3. The values of $-\nabla^2\rho$ and ρ for these carbon−carbon-bonded maximum charge concentrations in the four series of molecules follow the trend 2 > 1 > 3 > 4.

The ellipticities, $-\nabla^2\rho$, and ρ at the bond critical points for the halogen−carbon bonds are greater in series 2 than in series 3. Fluorine and chlorine produce the largest values of ρ and $-\nabla^2\rho$, respectively. These facts clearly show the delocalization of charge from the halogens to the sp^2 carbon. In the case of the carbon−carbon bond, the ellipticities at the bond critical point are greater in series 2 than in series 1 (also true for series 3 and series 4). These results also suggest an overlapping or delocalization of one of the nonbonded maximum charge concentrations of the VSCC of the halogens into the π cloud of the carbon−carbon double bond by a resonance effect. The ρ and $-\nabla^2\rho$ values exhibit the same behavior.

The populations of chlorine and bromine in series 2 are smaller than in series 3 (larger than 17 and 35, respectively). This suggests that the electron-withdrawing inductive effect of the halogens is larger than the donor resonance effect. However, the fluorine systems do not follow the same behavior. In the case of the carbon bonded to the halogens, the populations are always greater in series 2 than in series 3, which is consistent with the donor character of the halogen resonance effect. Furthermore, the delocalization indexes between the halogen and its bonded carbon are larger in series 2 than in series 3, which shows that the halogen resonance effect contributes to the sharing of electrons between the halogens and their bonded carbon.

The locations of the carbon−carbon link points of the VSCC in α- and β-naphthalene is slightly different than in benzene. The analysis of these link points in terms of $-\nabla^2\rho$ shows that electrophilic aromatic substitution is more favorable in α-fluoronaphthalene than in α-chloronaphthalene and α-bromonaphthalene. The same conclusion holds for the β-halonaphthalenes. Also, the results indicate a preference for C_1 over C_3 in the β-halonaphthalenes. All these results are consistent with experimental results.

In summary, we report several observations that are consistent with the presence of the halogen resonance effect in compounds where the halogen is bonded to a carbon−

carbon double bond. These observations include the missing nonbonded maximum charge concentration in the VSCC of the halogens, the increase of $-\nabla^2\rho$ and ρ in the bonded maximum charge concentrations in the VSCC of the halogens and in the VSCC of their respective bonded carbons, the electronic properties at the BCPs, the atomic populations, and the delocalization indexes. Furthermore, our observations are consistent with experimental results for electrophilic aromatic substitution in halonaphthalenes.

Acknowledgment. The authors wish to acknowledge the financial support of the Natural Sciences and Engineering Research Council of Canada.

References

(1) Dewar, M. J. S. *Mol. Struct. Energ.* **1988**, *6*, 1−61.

(2) Bader, R. F. W. *Atoms in Molecules—A Quantum Theory*; Oxford University Press: New York, 1990.

(3) Bader, R. F. W. *Chem. Rev.* **1991**, *91*, 893−928.

(4) Bader, R. F. W. *Can. J. Chem.* **1998**, *76*, 973−988.

(5) Bader, R. F. W.; Nguyen-Dang, T. *Adv. Quantum Chem.* **1981**, *14*, 63−123.

(6) Popelier, P. L. A. Atoms in Molecules. An Introduction; Prentice Hall: London, 2000.

(7) Matta, C. F.; Gillespie, R. J. *J. Chem. Educ.* **2002**, *79*, 1141−1151.

(8) Bader, R. F. W.; Stephens, M. E. *J. Am. Chem. Soc.* **1975**, *97*, 7391−7399.

(9) Fradera, X.; Austen, M. A.; Bader, R. F. W. *J. Phys. Chem. A* **1999**, *103*, 304−314.

(10) Austen, M. A. A New Procedure for Determining Bond Orders in Polar Molecules, with Applications to Phosphorus and Nitrogen Containing Systems. Ph.D. Thesis, McMaster University, Hamilton, Canada, 2003.

(11) Bader, R. F. W. *Inorg. Chem.* **2001**, *40*, 5603−5611.

(12) Matta, C. F.; Hernandez-Trujillo, J. *J. Phys. Chem. A* **2003**, *107*, 7496−7504.

(13) Bader, R. F. W.; Streitwieser, A.; Neuhaus, A.; Laidig, K. E.; Speers, P. *J. Am. Chem. Soc.* **1996**, *118*, 4959−4965.

(14) González, M. J.; Mosquera, R. *J. Phys. Chem. A* **2003**, *107*, 5361−5367.

(15) Okulik, N.; Peruchena, N. M.; Esteves, P. M.; Mota, C. J. A.; Jubert, A. *J. Phys. Chem. A* **1999**, *103* (42), 8491−8495.

(16) Okulik, N. B.; Sosa, L. G.; Esteves, P. M.; Mota, C. J. A.; Jubert, A. H.; Peruchena, N. M. *J. Phys. Chem. A* **2002**, *106* (8), 1584−1595.

(17) Grabowski, S. J. *J. Mol. Struct.* **2001**, *562* (1−3), 137−143.

(18) Grabowski, S. J. *J. Phys. Org. Chem.* **2003**, *16* (10), 797−802.

(19) Gilli, P.; Bertolasi, V.; Pretto, L.; Lycka, A.; Gilli, G. *J. Am. Chem. Soc.* **2002**, *124* (45), 13554−13567.

(20) Borbulevych, O. Y.; Clark, R. D.; Romero, A.; Tan, L.; Antipin, M. Y.; Nesterov, V. N.; Cardelino, B. H.; Moore, C. E.; Sanghadasa, M.; Timofeeva, T. V. *J. Mol. Struct.* **2002**, *604* (1), 73−86.

(21) Bader, R. F. W.; Chang, C. *J. Phys. Chem. A* **1989**, *93*, 2946−2956.

(22) Frisch, M. J.; Trucks, G. W.; Schlegel, H. B.; Scuseria, G. E.; Robb, M. A.; Cheeseman, J. R.; Montgomery, J. J. A.; Vreven, T.; Kudin, K. N.; Burant, J. C.; Millam, J. M.; Iyengar, S. S.; Tomasi, J.; Barone, V.; Mennucci, B.; Cossi, M.; Scalmani, G.; Rega, N.; Petersson, G. A.; Nakatsuji, H.; Hada, M.; Ehara, M.; Toyota, K.; Fukuda, R.; Hasegawa, J.; Ishida, M.; Nakajima, T.; Honda, Y.; Kitao, O.; Nakai, H.; Klene, M.; Li, X.; Knox, J. E.; Hratchian, H. P.; Cross, J. B.; Adamo, C.; Jaramillo, J.; Gomperts, R.; Stratmann, R. E.; Yazyev, O.; Austin, A. J.; Cammi, R.; Pomelli, C.; Ochterski, J. W.; Ayala, P. Y.; Morokuma, K.; Voth, G. A.; Salvador, P.; Dannenberg, J. J.; Zakrzewski, V. G.; Dapprich, S.; Daniels, A. D.; Strain, M. C.; Farkas, O.; Malick, D. K.; Rabuck, A. D.; Raghavachari, K.; Foresman, J. B.; Ortiz, J. V.; Cui, Q.; Baboul, A. G.; Clifford, S.; Cioslowski, J.; Stefanov, B. B.; Liu, G.; Liashenko, A.; Piskorz, P.; Komaromi, I.; Martin, R. L.; Fox, D. J.; Keith, T.; Al-Laham, M. A.; Peng, C. Y.; Nanayakkara, A.; Challacombe, M. W.; Gill, P. M.; Johnson, B.; Chen, W.; Wong, M. W.; Gonzalez, C.; Pople, J. A. *Gaussian 03*, revision B.03.; Gaussian Inc.: Pittsburgh, PA.

(23) Bader, R. F. W. *AIMPAC*. http://www.chemistry.mcmaster.ca/aimpac/.

(24) Biegler-König, F. W.; Bader, R. F. W.; Tang, T.-H. *J. Comput. Chem.* **1982**, *13*, 317−328.

(25) Matta, C. F. *AIMDELOC: Program to calculate AIM localization and delocalization indexes (QCPE0802)*; Quantum Chemistry Program Exchange: Indiana University, IN. http://qcpe.chem.indiana.edu/.

(26) Bader, R. F. W.; Gillespie, R. J.; MacDougall, P. J. *J. Am. Chem. Soc.* **1988**, *110*, 7329−7336.

(27) Bader, R. F. W.; Heard, G. L. *J. Chem. Phys.* **1999**, *111*, 8789−8798.

(28) Castillo, N.; Boyd, R. *J. Chem. Phys. Lett.* **2005**, *403*, 47−54.

(29) Popelier, P. L. A.; Burke, J.; Malcolm, N. O. J. *Int. J. Quantum Chem.* **2003**, *92*, 326−336.

(30) Taylor, R. *Electrophilic Aromatic Substitution*; John Wiley & Sons Ltd: England, 1990.

CT050238J